Improvement of OPED Algorithm by means of introducing an integration in the evaluation process

Oleg Tischenko^a, Yuan Xu^b, Christoph Hoeschen^a
^aGSF - National Research Center for Environment and Health, Institute for Radiation Protection, Ingolstaedter Landstrasse 1, D-85764 Neuherberg, Germany; ^b11B Deady Hall, Department of

Mathematics, University of Oregon, Eugene OR 97403 - 1222, USA

ABSTRACT

The tomographic method based on the orthogonal polynomial expansion on disc (OPED) was presented at SPIE conference of Medical Imaging 2006. We could show already some advantages compared to FBP as it is commonly used in today's CT systems. However, OPED did show for some specific cases some noise in the reconstructed images and even artefacts, mainly an aliasing. We have found that the OPED algorithm can be essentially improved by integrating the polynomial over the whole area belonging to the pixel instead of assigning to the whole pixel the polynomial value calculated just for one point of this pixel (typically bottom left). This advantageous implementation is effective in view of reduction of the aliasing artefacts and noise without affecting the resolution. This can be fulfilled effectively for OPED due to its simple structure.

Keywords: tomography, series expansion, OPED, aliasing

1. INTRODUCTION

1.1 OPED

The series expansion methods represent a special class of solutions for the problem of reconstructing a function f(x, y) from a limited set of its Radon projections $R_f(\varphi_v, t)$,

$$R_f(\varphi_v,t) = \int_{\mathbf{x}\cdot\mathbf{\varphi}_v=t} f(\mathbf{x},y)dxdy$$
,

where $\mathbf{x} \cdot \mathbf{\varphi} = x \cos \varphi + y \sin \varphi$. The of studying such solutions dates back to the article [1] where the solution appears as a result of imposing the norm minimum condition on the reconstruction of the function f supported in unit disc B. Other solutions of this problem under more general conditions were proposed since then by various authors (see e.g. [2], [3]). Detailed studying of this problem in terms of expansion of the function f in certain bases of orthogonal polynomials on unit disc was made in [4].

However, the series expansions methods have still not found its place in the practical tomography. We think that this is due to their seemingly complex structure. In fact, in [4] there was shown that the following compact and simple relation is valid:

$$f(x,y) \approx g(x,y) = \frac{1}{K} \sum_{\nu=0}^{K-1} \sum_{k=0}^{K-1} (k+1) U_k(\mathbf{x} \cdot \mathbf{\phi}_{\nu}) \frac{1}{\pi} \int_{-1}^{1} R_f(\varphi_{\nu},t) U_k(t) dt . \tag{1}$$

where $U_k(t)$ is Chebyshev polynomial of the second kind. The relation (1) becomes equality for the polynomials of degree $\leq K$. The right part of this formula has a very clear meaning. This is a partial sum of expansion of the function f in the basis of Chebyshev ridge polynomials of second kind on unit disc B. Therefore (1) was named OPED (Orthogonal Polynomial Expansion on Disc). It allows effective discretization and can be evaluated in a fast manner with a number of operation of the same order as for FBP (see [5], [6]). In [7] it was shown that OPED can be effectively used both in

Medical Imaging 2007: Physics of Medical Imaging, edited by Jiang Hsieh, Michael J. Flynn, Proc. of SPIE Vol. 6510, 65105I, (2007) · 1605-7422/07/\$18 · doi: 10.1117/12.711421

emission (PET) and transmission tomography, and in some cases has even advantages over FBP in terms of mean error, norm deviation and Hilbert cosine.

1.2 Representation of reconstruction

The choice of the evaluation grid is important for representing the reconstruction. In the 2D case, this is normally a $N \times N$ rectangular grid, and the only question is how large the number N must be. Very big N leads to higher evaluation cost. Besides, if N becomes larger the non-interest features such as streak artifacts or inevitable oscillations in the regions which are supposed to be constant become more prominent. Indeed, because of these noisy features, the reconstruction has to be sufficiently small in order to allow an adequate assessment in diagnostics. On the other side, according to the sampling theory, for adequate representation of a signal, its Nyquist frequency must be taken into account. Otherwise there is a risk to represent the signal with aliasing. Therefore the optimal size of the evaluation grid in tomography has to be chosen with consideration of the Nyquist frequency of the reconstruction. The latter is determined by the resolution of detectors participating in data collection and the number of read-out positions e.g. during one cycle of gantry rotation. However, in the practice one tends to evaluate the reconstructing function at the sampling rate which lies under the Nyquist level. In the "lucky" cases this leads to an image with somewhat higher visual quality. But even in the presence of the aliasing there exist different approaches to reduce the alias-effect in the reconstruction. In some cases, anti-aliasing procedures are retroactive, i.e. they are applied to the results of the evaluation on some primary grid. The retroactive procedures inevitably affect the reconstruction so that the chosen grid is no more optimal for the final representation.

Here we propose an efficient way to obtain the reconstructions which are free of aliasing and still optimal for the chosen evaluation gird.

2. METHODS

An efficient way of representing the reconstruction which is free of aliasing and, at the same time, is optimal for the chosen evaluation grid can be described as follows. Let B denote the unit disc in the plane, and let the reconstructing function g(x,y) be known for all $(x,y) \in B$. Instead of representing g by its samples $g(x_i,y_j)$, it can be represented by its weighted averages $g_{i,j}$,

$$g_{i,j} = g * e[x_i, y_j] = \langle g, e_{i,j} \rangle, \qquad (2)$$

where '*' means the convolution with a kernel e(x, y), and $e_{i,j}(x, y) = e(x_i - x, y_j - y)$. Properties of the kernel function can be chosen ad hoc. Note that the smoothing of type (2) differs radically from retroactive smoothing of samples $g(x_i, y_j)$. The desired representation of g(x, y) is determined by a view of the kernel function and the size of its support. The latter has to be optimal for the chosen evaluation grid.

For OPED the task (2) is reduced to the calculation of coefficients

$$\left\langle U_k, e_{i,j} \right\rangle = \int_{B \cap B_{i,j}^e} U_k(x \cos \varphi + y \sin \varphi) e_{i,j}(x, y) dx dy \tag{3}$$

where $B_{i,j}^e$ is the support of the kernel e. If functions $e_{i,j}$ generate a basis in the subspace $E \subset L_2(B)$, then one may speak of the representation of the reconstructing function g(x,y) in this basis. If $e_{i,j}$ are orthonormal, then one can speaks of an orthogonal projection of g onto the subspace E. Except for removing the aliasing, this procedure has other advantages. First of all, it reduces the noise amplitude of g. Besides, one can reduce the time cost needed normally for additional antialiasing procedures.

In this paper we study a special case where the kernel function e is a box function with the support of size which is equal to the area of the pixel, i.e.

$$e_{i,j}(x,y) = \begin{cases} \frac{N^2}{4}, & \text{if } \frac{i-N}{N} \le x \le \frac{i-N+1}{N}, \frac{j-N}{N} \le y \le \frac{j-N+1}{N} \\ 0, & \text{otherwise} \end{cases}$$
 (4)

That is, we represent the reconstructing function g(x, y) by its averages over the pixels each side of size $\Delta = 2/N$.

2.1 Integrating over pixels

As it was already mentioned, the procedure of averaging is reduced to computing coefficients defined by (3) with kernels $e_{i,j}$ defined in (4). This results in calculating the integral

$$\int_{y_{i-1}}^{y_{i+1}} \int_{x_{i}}^{y_{i+1}} U_k(\mathbf{x} \cdot \mathbf{\phi}) dx dy . \tag{5}$$

Using the equality

$$U_{k}(\mathbf{x} \cdot \mathbf{\phi}) = \frac{1}{(k+1)\sin 2\varphi} \frac{\partial^{2}}{\partial x \partial y} \left[\frac{T_{k+2}(\mathbf{x} \cdot \mathbf{\phi})}{k+2} - \frac{T_{k}(\mathbf{x} \cdot \mathbf{\phi})}{k} \right] = \frac{1}{(k+1)\sin 2\varphi} \frac{\partial^{2} \rho_{k}(\mathbf{x} \cdot \mathbf{\phi}_{v})}{\partial x \partial y}, \tag{6}$$

(see Appendix A), one finds that

$$\int_{y_{j}}^{y_{j+1}} \int_{x_{i}}^{x_{i+1}} U_{k}(\mathbf{x} \cdot \mathbf{\phi}_{v}) dx dy = \frac{1}{(k+1)\sin 2\varphi} \left[\left[\rho_{k}(\mathbf{x} \cdot \mathbf{\phi}_{v}) \right]_{x_{i}}^{x_{i+1}} \right]_{y_{j}}^{y_{j+1}}, \tag{7}$$

where $[f(t)]_{t_1}^{t_2}$ means as usually the difference $f(t_2) - f(t_1)$.

In order to compute all coefficients $\langle g, e_{i,j} \rangle$, it is necessary to evaluate the expression

$$I(x,y) = \frac{1}{\Delta^2} \frac{1}{K} \sum_{v=0}^{K-1} \sum_{k=0}^{K-1} \frac{\rho_k(\mathbf{x} \cdot \mathbf{\phi}_v)}{\sin 2\varphi_v} \frac{1}{\pi} \int_{-1}^{1} R_f(\varphi_v, t) U_k(t) dt$$
 (8)

in all knots of the evaluation grid. Indeed, if I(x, y) is knows for all pairs x_i, y_j , then

$$\langle g, e_{i,j} \rangle = I(x_{i+1}, y_{i+1}) - I(x_i, y_{i+1}) - I(x_{i+1}, y_i) + I(x_i, y_i).$$
 (9)

Note that the cost of evaluation of (8) is the same as for the evaluation of (1). The desired representation is then

$$g = \sum_{i=0}^{N-1} \sum_{i=0}^{N-1} \langle g, e_{i,j} \rangle e_{i,j} . \tag{10}$$

2.2 Numerical stability

In expression (8) there is $\sin 2\varphi_v$ in the denominator which can be either zero or very close to zero. Besides, there is a factor 1/k in (6), and k can be zero as well. These numerical instabilities can be treated as follows. For the simplicity of notations in the following, let

$$S_{k,\nu} = \frac{1}{\pi} \int_{-1}^{1} R_f(\varphi_{\nu}, t) U_k(t) dt.$$

Then

$$I(x,y) = \frac{1}{\Delta^2} \frac{1}{K} \sum_{v=0}^{K-1} \sum_{k=0}^{K-1} \frac{\rho_k(x \cos \varphi_v + y \sin \varphi_v) S_{k,v}}{\sin 2\varphi_v}.$$
 (11)

Denote by Φ_0 the set of all indices v such that $\sin 2\varphi_v = 0$. Then I(x, y) can be written as a sum of two terms,

$$I(x,y) = I_1(x,y) + \frac{1}{\Delta^2} \frac{1}{K} \sum_{v=0, k=0}^{K-1} \frac{\rho_k(x \cos \varphi_v + y \sin \varphi_v) S_{k,v}}{\sin 2\varphi_v},$$
(12)

where the second term is numerically unstable. The contribution of this term in (9) is estimated in Appendix C. There it is shown that if $\Phi_0 = \{v : \sin 2\varphi_v = 0\}$, then

$$\langle g, e_{i,j} \rangle = I_1(x_{i+1}, y_{i+1}) - I_1(x_i, y_{i+1}) - I_1(x_{i+1}, y_i) + I_1(x_i, y_i) + I_1(x_i, y_i) + \frac{1}{K} \left[\frac{1}{\Delta} \sum_{k=1}^{K-1} (T_k(x_{i+1}) - T_k(x_i)) C_k^x + \frac{1}{\Delta} \sum_{k=1}^{K-1} (T_k(y_{i+1}) - T_k(y_i)) C_k^y \right].$$
(13)

The case of zero index k is treated distinctly. Let

$$I(x,y) = \frac{1}{\Delta^2} \frac{1}{K} \sum_{\nu=0}^{K-1} \sum_{k=1}^{K-1} \frac{\rho_k (x \cos \varphi_\nu + y \sin \varphi_\nu) S_{k,\nu}}{\sin 2\varphi_\nu} + \frac{1}{\Delta^2} \frac{1}{K} \sum_{\nu=0}^{K-1} \frac{\rho_0 (x \cos \varphi_\nu + y \sin \varphi_\nu) S_{0,\nu}}{\sin 2\varphi_\nu} . \tag{14}$$

Denoting by $I_2(x, y)$ the second term in (14), one can find directly that

$$I_2(x_{i+1}, y_{i+1}) - I_2(x_i, y_{i+1}) - I_2(x_{i+1}, y_i) + I_2(x_i, y_i) = \frac{1}{K} \sum_{i=0}^{K-1} S_{0,v}.$$
 (15)

The whole algorithm can therefore be formulated as follows. Let

$$J(x,y) = \frac{1}{\Delta^{2}} \frac{1}{K} \sum_{v \notin \Phi_{v}} \sum_{k=1}^{K-1} \frac{\rho_{k}(x \cos \varphi_{v} + y \sin \varphi_{v}) S_{k,v}}{\sin 2\varphi_{v}} = \frac{1}{\Delta^{2}} \frac{1}{K} \sum_{v \notin \Phi_{v}} \sum_{k=1}^{K-1} \left[\frac{T_{k+2}(\mathbf{x} \cdot \mathbf{\varphi}_{v})}{k + 2} - \frac{T_{k}(\mathbf{x} \cdot \mathbf{\varphi}_{v})}{k} \right] \frac{S_{k,v}}{\sin 2\varphi_{v}}$$

then

$$\langle g, e_{i,j} \rangle = J(x_{i+1}, y_{i+1}) - J(x_i, y_{i+1}) - J(x_{i+1}, y_i) + J(x_i, y_i) + r_{i,j},$$
 (16)

where

$$r_{i,j} = \frac{1}{K} \left[\sum_{\nu=0}^{K-1} S_{0,\nu} + \frac{1}{\Delta} \sum_{k=1}^{K-1} (T_k(x_{i+1}) - T_k(x_i)) C_k^x + \frac{1}{\Delta} \sum_{k=1}^{K-1} (T_k(y_{i+1}) - T_k(y_i)) C_k^y \right]. \tag{17}$$

The approximation (16) is stable and can be computed in a fast manner.

2.3 Fast reconstruction

As it follows from (16), one needs to evaluate $J(x_i, y_j)$ and $r_{i,j}$ for each grid point (x_i, y_j) lying inside of the unit disc. If the matrix $T_k(-1+j\Delta)$, $1 \le k < K$, $0 \le j < N$ is known in advance, then the cost of evaluation of $r_{i,j}$ is O(K) multiplications. For the following let us introduce the family of functions

$$g_{\nu}(t) = \sum_{k=1}^{K-1} \frac{S_{\nu,k}}{\sin 2\varphi_{\nu}} \rho_{k}(t). \tag{18}$$

Then

$$J(x,y) = \frac{1}{\Delta^2} \frac{1}{K} \sum_{v \neq \phi_0} g_v (x \cos \varphi_v + y \sin \varphi_v).$$

The idea of fast reconstruction is to evaluate functions $g_v(t), v \notin \Phi_0$ first in points t_j , $-1 \le t_1 < t_2 < ... < t_M \le 1$, and then to estimate $g_v(x \cos \varphi_v + y \sin \varphi_v)$ interpolating known values $g_v(t_j)$.

For the evaluation of $g_v(t)$, one needs to compute the matrix $S_{k,v}$. The integral

$$S_{k,\nu}(t) = \frac{1}{\pi} \int_{-1}^{1} R_f(\varphi_{\nu}, t) U_k(t) dt$$
 (19)

can be represented in the form

$$S_{k,v} = \frac{1}{\pi} \int_{0}^{\pi} R_f(\varphi_v, \cos \psi) \sin(k+1) \psi d\psi.$$
 (20)

This is done through the change $t = \cos \psi$ in (19). In many practical cases the integral (20) can be approximated efficiently with Gaussian quadrature:

$$S_{k,\nu} \approx \frac{1}{K} \sum_{i=0}^{K-1} R_f(\varphi_{\nu}, \cos \psi_j) \sin(k+1) \psi_j , \qquad (21)$$

where ψ_j is equally spaced between 0 and π . (In fact, the Gaussian quadrature is exact for trigonometric polynomials of degree $\leq 2N$ (see [8])). In this case the matrix $S_{k,v}$ can be evaluated in a fast manner by means of sine transform.

The number of operations necessary for the evaluation of the matrix $S_{k,v}$ is of the order $K^2 \log K$. For the evaluation of functions $g_v(t)$ in M different points t_j , one needs $O(K^2M)$ operations. Finally, if the size of evaluation grid for the reconstruction is chosen to be $K \times K$, then the whole number of operations necessary for the reconstruction is of the order $O(K^2(M + \log K))$. This is of the same order as for the reconstruction with FBP. The similar scheme allowing to accelerate the evaluation of (1) without averaging was proposed in [5].

3. RESULTS

The method was tested on data produced analytically for the Shepp and Logan phantom. Exact characteristics of this phantom were published in [9]. The data were collected over the lines $x \cos \varphi_y + y \sin \varphi_y = t_i$ where

$$\varphi_v = \frac{2\pi}{K}v, v = 0, 1, ..., K - 1 \text{ and } t_j = \cos\psi_j, \ \psi_j = \left(\frac{1}{2} + j\right)\frac{\pi}{K}$$

with K = 1001. The reconstructions from these data were performed twice on a 256×256 grid, once with averaging and once via direct evaluation of the formula (1) in the grid points. Both images are represented in Figure 1. The aliasing artifacts are clearly seen in the reconstruction performed without averaging (right image). Besides, the typical "step edge" artifact is also visible in this image. In contrary the reconstruction implying the averaging procedure is free from these artifacts.

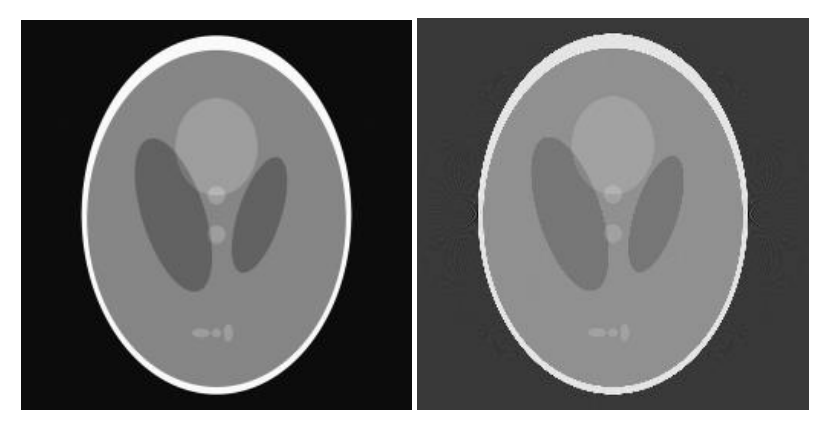


Fig.1. Two reconstructions made with averaging over pixel (left) and without (right).

The profiles of the central vertical slice of both reconstructions are represented in the plots of Figure 2 and 3. The plot of Figure 2 shows the profile of the left image of Figure 1. Figure 3 shows the profile of the right image of Figure 1. One can see that the profile of the image implying the averaging is constant in the regions which have to be constant. At the same time, the resolution of averaged image was not suffered.

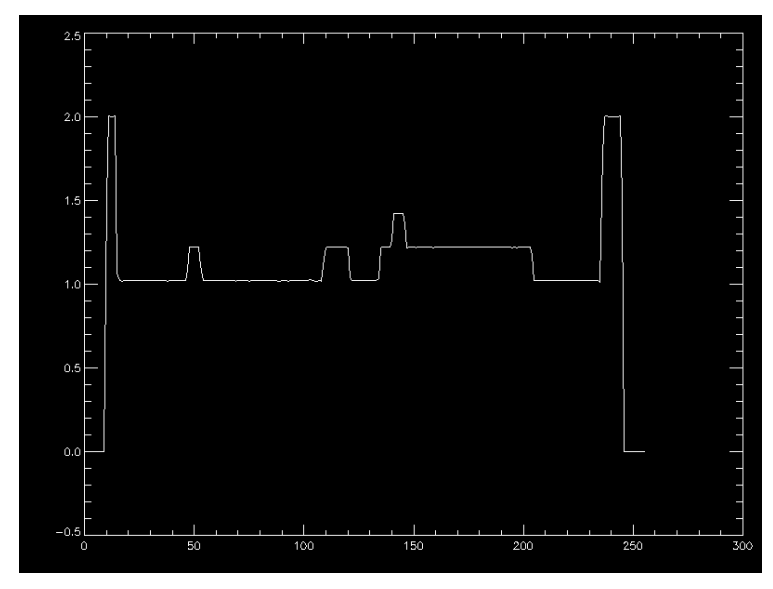


Fig.2. Profile of central vertical slice of the left image of Figure 1

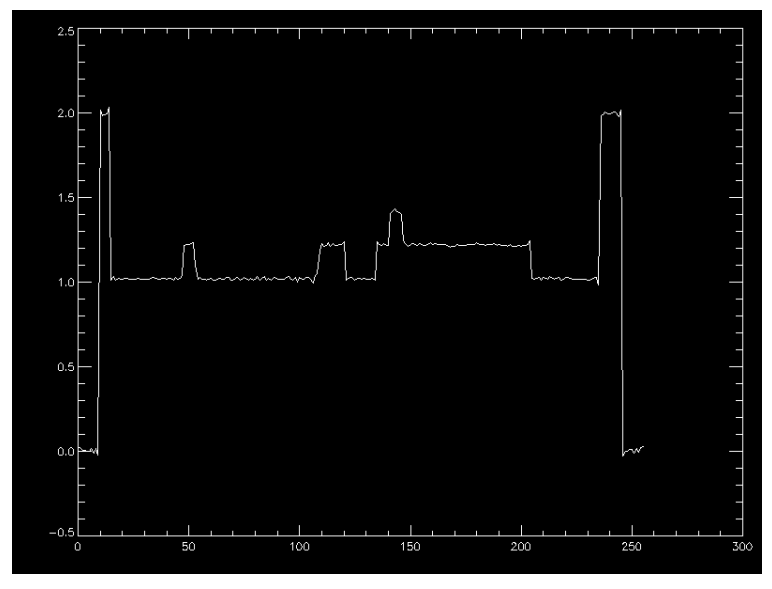


Fig.3. Profiles of central vertical slice of the right image of Figure 1.

4. CONCLUSIONS

We have shown that the operation of averaging over pixels of the reconstructing function g(x, y) can be effectively performed for OPED algorithm. Such an averaging differs from the averaging made retrospectively for the samples $g(x_i, y_i)$ used sometimes in order to reduce the undesired effects such as e.g. aliasing. The averaging over pixels has a number of advantages. The most apparent one is that the averaged representation is free of aliasing. Another advantage is that the smoothness of edges of structures in the reconstruction is kept. The averaging over pixels has also the ability to reduce the amplitude of noise if the size of the pixel is bigger than the sampling rate corresponding to Nyquist frequency of the reconstruction.

5. APPENDIX

5.1 Appendix A

Let

$$\rho_k(t) = \frac{T_{k+2}(t)}{k+2} - \frac{T_k(t)}{k}, \quad t = x\cos\theta + y\sin\theta . \tag{A1}$$

Then

$$\frac{\partial^2 \rho_k(t)}{\partial x \partial y} = \sin \theta \cos \theta \frac{d^2 \rho}{dt^2} \,. \tag{A2}$$

Taking into account the following two equalities

$$\frac{dT_{k+1}(t)}{dt} = (k+1)U_k(t), \tag{A3}$$

$$U_{k+1}(t) - U_{k-1}(t) = 2T_{k+1}(t), \tag{A4}$$

one finds that

$$\frac{d^2\rho(t)}{dt^2} = \frac{d}{dt}(U_{k+1}(t) - U_{k-1}(t)) = 2\frac{d}{dt}T_{k+1}(t) = 2(k+1)U_k(t),\tag{A5}$$

from which it follows that

$$\frac{1}{k+1} \frac{1}{\sin 2\theta} \frac{\partial^2 \rho(t)}{\partial x \partial y} = U_k(t). \tag{A6}$$

5.2 Appendix B

Representing Chebyshev polynomial $T_k(t)$ of the fist kind with first two terms of its Taylor expansion and using the formula (A3), one finds that by $\varepsilon \to 0$

$$T_{k}(t+\varepsilon) = T_{k}(t) + \frac{dT_{k}(t)}{dt}\varepsilon + O(\varepsilon^{2}).$$
(B1)

Using (A4), one obtains that for the function ρ_k defined in (A1), the approximation

$$\rho_k(t+\varepsilon) \approx \rho_k(t) + 2\varepsilon T_k(t)$$
(B2)

is valid.

5.3 Appendix C

Let

$$J(x,y) = \frac{1}{\Delta^2} \frac{1}{K} \sum_{v \in 0} \frac{1}{\sin 2\varphi_v} \sum_{k=0}^{K-1} \rho_k (x \cos \varphi_v + y \sin \varphi_v) S_{k,v},$$
 (C1)

where the set Φ_0 is the set of all indices v such that $|\sin 2\varphi_v| \approx 0$. The function ρ_k is defined in (A1). One has to estimate the value

$$J(x_{i+1}, y_{i+1}) - J(x_i, y_{i+1}) - J(x_{i+1}, y_i) + J(x_i, y_i).$$
(C2)

The following decomposition of Φ_0 will be useful in the following: $\Phi_0 = \Phi_0^{+x} \bigcup \Phi_0^{-x} \bigcup \Phi_0^{-y} \bigcup \Phi_0^{-y}$. For the indices from Φ_0^{+x} , the inequality $\left| \varphi_v \right| \le \varepsilon$ is valid, while for the indices from Φ_0^{-x} , $\left| \pi - \varphi_v \right| \le \varepsilon$. In the same manner, if $v \in \Phi_0^{+y}$ then $\left| \varphi_v - \pi/2 \right| \le \varepsilon$, and if $v \in \Phi_0^{-y}$ then $\left| \varphi_v - 3\pi/2 \right| \le \varepsilon$. Using (B2), it is easy to find that by $\varepsilon = 0$ the value (C2) takes the view

$$\begin{split} J\!\!\left(x_{i+1},y_{j+1}\right) - J\!\!\left(x_{i},y_{j+1}\right) - J\!\!\left(x_{i},y_{j}\right) + J\!\!\left(x_{i},y_{j}\right) &= \\ &= \frac{1}{\Delta^{2}} \frac{1}{K} \sum_{v \in \Phi_{0}^{+x}} \left(y_{j+1} - y_{j}\right) \!\! \sum_{k=0}^{K-1} \!\! \left(T_{k}\!\!\left(x_{i+1}\right) - T_{k}\!\!\left(x_{i}\right)\!\right) \!\! S_{k,v} + \frac{1}{\Delta^{2}} \frac{1}{K} \sum_{v \in \Phi_{0}^{-x}} \!\! \left(y_{j+1} - y_{j}\right) \!\! \sum_{k=0}^{K-1} \!\! \left(T_{k}\!\!\left(-x_{i+1}\right) - T_{k}\!\!\left(-x_{i}\right)\!\right) \!\! S_{k,v} + \\ &+ \frac{1}{\Delta^{2}} \frac{1}{K} \sum_{v \in \Phi_{0}^{+y}} \!\! \left(x_{i+1} - x_{i}\right) \!\! \sum_{k=0}^{K-1} \!\! \left(T_{k}\!\!\left(y_{j+1}\right) - T_{k}\!\!\left(y_{j}\right)\!\right) \!\! S_{k,v} + \frac{1}{\Delta^{2}} \frac{1}{K} \sum_{v \in \Phi_{0}^{+y}} \!\! \left(x_{i+1} - x_{i}\right) \!\! \sum_{k=0}^{K-1} \!\! \left(T_{k}\!\!\left(-y_{j+1}\right) - T_{k}\!\!\left(-y_{j}\right)\!\right) \!\! S_{k,v}. \end{split}$$

Finally, taking into account that $T_k(-t) = (-1)^k T_k(t)$ and that $T_0(t) \equiv 1$, one finds that

$$J(x_{i+1}, y_{j+1}) - J(x_i, y_{j+1}) - J(x_{i+1}, y_j) + J(x_i, y_j) =$$

$$= \frac{1}{K} \left[\frac{1}{\Delta} \sum_{k=1}^{K-1} (T_k(x_{i+1}) - T_k(x_i)) C_{k,v}^x + \frac{1}{\Delta} \sum_{k=1}^{K-1} (T_k(y_{j+1}) - T_k(y_j)) C_{k,v}^y \right]$$
(C3)

where

$$\begin{split} &C_k^x = \sum_{v \in \Phi_0^{+x}} S_{k,v} + \sum_{v \in \Phi_0^{-x}} (-1)^k S_{k,v}, \\ &C_k^y = \sum_{v \in \Phi_0^{+y}} S_{k,v} + \sum_{v \in \Phi_0^{-y}} (-1)^k S_{k,v}. \end{split}$$

REFERENCES

- 1. B. F. Logan and L. A. Shepp, "Optimal reconstruction of a function from its projections", *Duke Math. J.*, **42**:4, 645-659 (1975).
- 2. M. E. Davison and F. A. Gruenbaum, "Tomographic reconstruction with arbitrary directions", *Comm. Pure Appl. Math.*, **34**, 77-120 (1981).
- 3. H. H. Barrett und K. J. Meyers, *Foundations of image science*, John Willey & Son, Inc., Hoboken, New Jersey 2004.
- 4. Y. Xu, "A direct approach to the reconstruction of images from Radon projections", *Adv. in Applied Math.*, **36**, 388-420 (2006).
- 5. Y. Xu and O. Tischenko, "Fast OPED algorithm for reconstruction of images from Radon projections", submitted
- 6. Y. Xu, O. Tischenko and C. Hoeschen, "A new reconstruction algorithm for Radon data", *Proc. SPIE*, **6142**, 791-798 (2006).
- 7. O. Tischenko, Y. Xu, H. Schlattl and C. Hoeschen, "An alternative tomographic reconstruction algorithm", submitted.
- 8. Ch. F. Dunkl and Y. Xu, *Orthogonal polynomials of several variables*, Cambridge University Press, Cambridge, 2001.
- 9. L. A. Shepp and B. F. Logan, "The Fourier reconstruction of a head section", *IEEE Trans. Nucl. Sci.*, **21**, 21-23 (1974)